



Published in final edited form as:

Burns. 2010 March ; 36(2): 232–238. doi:10.1016/j.burns.2009.02.019.

Age-Dependent Differences of Interleukin-6 Activity in Cardiac Function after Burn Complicated by Sepsis¹

Lin Wang², Jiexia Quan², William E. Johnston², David L. Maass³, Jureta W. Horton³, James A. Thomas⁴, and Weike Tao²

² Department of Anesthesiology and Pain Management, University of Texas Southwestern Medical Center at Dallas, Dallas, TX 75390-9068

³ Department of Surgery, University of Texas Southwestern Medical Center at Dallas, Dallas, TX 75390-9068

⁴ Department of Pediatrics, University of Texas Southwestern Medical Center at Dallas, Dallas, TX 75390-9068

Abstract

Interleukin (IL)-6 is a pleiotropic cytokine that is activated after acute injuries, and plays an important role during aging. We aim to define the role of IL-6 on myocardial dysfunction following a 40% total body surface area burn followed by late (7 days) *S. pneumoniae* sepsis (burn plus sepsis) in 2- and 14-month-old wild type and IL-6^{-/-} mice. We measured global hemodynamic and cardiac contractile function with left ventricular pressure-volume analysis 24 hours after sepsis induction, and measured phosphorylated signal transducer and activator of transcription 3 (p-STAT-3), tumor necrosis factor (TNF)- α , and IL-1 β in the heart with Western blot analysis. We also measured mRNA expression of IL-6, TNF- α , and IL-1 β . Sham injured mice did not manifest any appreciable level of p-STAT-3 or functional deficiencies regardless of age or presence of the IL-6 gene. Burn plus sepsis injury was associated with a significant deterioration of global hemodynamic and cardiac contractile function in WT mice in both age groups. This dysfunction was attenuated by IL-6 deficiency at age 2 months, but accentuated at age 14 months. Aging was associated with an increase in mRNA expression of IL-6 (WT mice), TNF- α , and IL-1 β (all mice). At age 14 months, IL-6 deficient mice exhibited a greater TNF- α mRNA expression than the wild type mice. We conclude aging is associated with altered cytokine gene transcription, and burn plus sepsis injury further intensifies such gene responses. IL-6 deficiency does not abrogate STAT-3 phosphorylation and it may enhance expression of other inflammatory cytokines. The differential effects of IL-6 deficiency on the cardiac function in young and aging mice cannot be explained by cytokine gene expression alone, and require further studies.

¹This work is supported by the National Institute of General Medical Sciences 1K08GM073141 (W.T.) and 5P50GM21681-41 (J.W.H. and J.A.T.). This work was presented at the 31st Annual Conference on Shock, June 28 – July 2, 2008, Cologne, Germany. This paper is in loving memory of Jureta W. Horton, our inspirational mentor, supporter, and dear friend.

Address Correspondence Requests to: Weike Tao, Department of Anesthesiology and Pain Management, the University of Texas Southwestern Medical Center at Dallas, 5323 Harry Hines Blvd., Dallas, TX 75390-9068. Phone: 214-648-4840; Fax: 214-648-2229; email: weike.tao@utsouthwestern.edu.

Conflict of Interest Statement

There is no conflict of interest in the paper "Age-Dependent Differences of Interleukin-6 Activity in Cardiac Function after Burn Complicated by Sepsis" for consideration of publication in Burns.

Publisher's Disclaimer: This is a PDF file of an unedited manuscript that has been accepted for publication. As a service to our customers we are providing this early version of the manuscript. The manuscript will undergo copyediting, typesetting, and review of the resulting proof before it is published in its final citable form. Please note that during the production process errors may be discovered which could affect the content, and all legal disclaimers that apply to the journal pertain.

Keywords

interleukin-6; cytokines; burn; sepsis; heart; aging

Introduction

Interleukin (IL)-6 is a key regulatory cytokine in the acute phase reaction following injuries such as burn and sepsis. Despite controversies regarding its role in the inflammatory response, there is evidence that IL-6 potentiates the inflammatory process and participates in tissue injury and cell death [1] [2]. In addition, IL-6 production is increased with aging. Blood levels of IL-6 are undetectable in young individuals but start to rise after age 50 [3]. A longitudinal community study in people between 55 and 95 years has shown linear increases of blood IL-6 levels with age [4]. High levels of IL-6 and C-reactive protein are powerful predictors for all-cause mortality [5].

Burn injury is a specific threat to the elderly, as society ages and more older people continue living independently [6]. Old age has long been recognized as a risk factor for poor outcome after burn, with patients older than 65 years suffering 5–6 times the mortality and requiring twice the length of hospital stay compared to the average aged adult [7]. A recent review also showed a marked mortality increase in burn patients 65 years and older, and the survival in this population has not improved as much as it has in younger patients despite progresses made in burn care over time [8]. In fact, an analysis from our own institutional data indicate that an age of 50 years or older is an independent risk factor for severe multi-organ dysfunction after burn [9].

The link between increased IL-6 and poor outcome after burn with aging remains to be determined. Cardiac dysfunction has been demonstrated in numerous studies after acute injuries including burn and sepsis. In a review of 1,674 patients with severe burn, cardiac complications were the second most common organ-related cause of mortality [8]. In our *in vitro* study, IL-6 potentiated the myocardial depressive effects of tumor necrosis factor (TNF)- α and IL-1 β [10]. More recently, we demonstrated *in vivo* the role of IL-6 in exacerbating myocardial inflammation and contractile dysfunction after burn complicated by sepsis [11]. Goal-directed treatment of burn [12] and sepsis [13] with fluid resuscitation aimed at restoring hemodynamic function has shown survival benefits. Based on these findings, we hypothesize that age-associated IL-6 increases contribute to cardiac contractile dysfunction, which may lead to the development of multiorgan dysfunction associated with the poorer outcome seen in older burn patients. In this study, we used wild type (WT) and IL-6 knockout (IL-6^{-/-}, KO) mice at 2 months (MO) and 14 MO of age to analyze global hemodynamic and cardiac contractile function in our clinically relevant model of cutaneous burn complicated by pneumonia with sepsis [14,15]. Although 14 MO mice correspond roughly with the human age of 45–50 years [16], which is by no means considered “old,” our goal is to study mechanisms contributing to the poor outcome after burn at age 50 years while avoiding possible influence of excessive co-morbidities associated with older ages.

Materials and Methods

Animals

Male wild type (WT, C57BL/6J) and IL-6 knockout (IL-6 KO, C57BL/6J-Il6^{tm1Kopf}) mice were obtained from the Jackson Laboratory (Bar Harbor, ME) at age 2 MO and 6–8 MO. Older mice were further aged on campus to the target age of 14 MO with similar housing and feeding conditions to the vendor. A total of 10–14 mice were used in each of the 2- or 14-MO, WT or KO, sham or burn complicated by sepsis (B+S) groups, with a total of eight groups. For

functional analysis, we combined our current data with those in the previous study [11] for the 2 MO WT and KO mice (the procedure was performed by the same operator), but all 14 MO mice were new to the study. All experimental procedures were reviewed and approved by the Institutional Animal Care and Use Committee and all animals were handled in accordance with guidelines outlined in the “Guide for the Care and Use of Laboratory Animals” as published by the American Physiology Society and the National Institutes of Health.

The burn complicated by sepsis (B+S) injury model

We have previously characterized global hemodynamic and cardiac contractile dysfunction in mice [17]. Burn complicated by sepsis (B+S) causes the maximum myocardial depression, and this compound injury closely represents the clinically relevant scenario in which a septic complication is associated with 80% of multi-organ dysfunction syndrome and therefore poses the greatest threat to burn victims [9]. Accordingly, we have chosen to use the B+S injury model in our current study.

Burn Injury—We used our *murine* model of 40% total body surface area (TBSA) contact burn as previously described [14,18]. After the body weight was obtained, mice were placed in a plastic chamber insufflated with 2.5% isoflurane in oxygen. After loss of consciousness, the skin was clipped, shaved, and washed with alcohol. Contact burn was induced by brass probes heated to 100 °C in boiling water for 30 minutes. The size of the probes and number of contact areas were selected based on the animal’s size to achieve a 40% TBSA burn area, which covered the entire dorsal area below the neck. Thorough heating of probes and solid contacts with skin were ensured to induce a complete third-degree burn without any margins of first- or second-degree burn. This previously described model of injury was confirmed by histology [18]. After the burn injury, animals were given 4 mL/kg/%TBSA intraperitoneal lactated Ringer’s solution for resuscitation, and 0.05 mg/kg buprenorphine was given every 12 hrs after burn for pain control. Mice were allowed to recover in cages placed on warming blankets with free access to food and water. Sham burn mice underwent the same anesthesia and skin preparation, but were only exposed to brass probes heated to 37 °C.

Streptococcus pneumoniae Sepsis—*Streptococcus pneumoniae* type 3 (ATCC 6303) was obtained from the American Type Culture Collection (Rockville, MD) and inoculated into the trachea seven (7) days after the initial burn injury as previously described [14]. Briefly, mice were anesthetized with isoflurane as described above. They were placed in a supine position, and the area over the trachea was prepared with povidone-iodine and alcohol. Using sterile instruments, a midline incision was made over the trachea; the trachea was identified and isolated via blunt dissection. A 0.1 mL aliquot of bacterial suspension containing 1×10^5 CFU of *S. pneumoniae* was injected directly into the trachea using a 31-gauge needle. The concentration of the bacteria was determined by densitometry and confirmed with bacterial culture. Sham mice received the 0.1 mL of phosphate buffered solution as vehicle without bacteria. After the endotracheal instillation, mice were placed in a 30° head-up position for five minutes to facilitate entry of bacteria into the lungs. The wound was closed with 6-0 polypropylene sutures. After receiving 2 mL of intraperitoneal lactated Ringer’s solution for fluid resuscitation, mice were allowed to recover from anesthesia. This model of pneumonia-related sepsis was confirmed 24 hrs after bacterial challenge by positive blood cultures ($> 2 \times 10^3$ CFU) and bronchial lavage cultures ($> 1 \times 10^6$ CFU) of the original bacterial strain.

Hemodynamic and cardiac function assessments

We used our previously established method of hemodynamic and cardiac contractile function measurements with internal carotid artery cannulation and pressure-volume analysis of the left ventricle (LV) [11,14,17,19,20]. The left carotid artery was cannulated with fluid-filled tubing connected to a pressure transducer (BLPR, WPI, Sarasota, FL) and the LV pressure-volume

data were collected with a 1.4 Fr. conductance catheter (SPR 839, Millar Instruments, Houston, TX). Steady state hemodynamics was measured, followed by contractility parameters with preload reduction transient (1–2 seconds) inferior vena cava (IVC) occlusion while suspending mechanical ventilation. Data were digitally converted and displayed using Chart software (v. 4.12, ADInstruments, Castle Hill, Australia). Hemodynamic and contractility measurements were made at a constant isoflurane concentration of 1.5% and a standard preload of a left ventricular end-diastolic volume of 15–18 relative volume units (RVU) [17]. Steady-state hemodynamic measurements included mean arterial pressure (MAP), heart rate (HR), stroke volume (SV), along with cardiac output (CO) and systemic vascular resistance (SVR) as calculated variables. Variables obtained during IVC occlusion included left ventricular end-systolic pressure-volume relationship (ESPRV), preload-recruitable stroke work (PRSW), time-varying maximum elastance (E_{max}) [14,17]. The slopes of ESPVR and PRSW represented the end-systolic pressure and stroke work of the left ventricle generated in response to a changing left ventricular end-diastolic volume caused by transient IVC occlusion. Likewise, E_{max} was the maximum left ventricular pressure/volume response at varying preload [21]. Data were analyzed with pressure-volume analysis software (PVAN ver. 3.1, Millar Instruments).

Cardiac tissue Western blot analysis of signal transducer and activator of transcription 3 (STAT-3), phosphorylated STAT-3 (p-STAT-3) and cytokines

To ensure accuracy of the hemodynamic and cardiac function assessment, no blood samples were drawn for cytokine measurements using ELISA. At the end of the hemodynamic and cardiac contractility experiment, the heart was rapidly excised, rinsed in 4 °C saline and stored at –80°C. Frozen heart tissues were homogenized in ice-cold lysis buffer (0.5 g tissue/mL) containing 10 mM HEPES (pH 7.4), 2 mM EDTA, 0.1% CHAPS, 5 mM DTT, 1 mM PMSF, and one Mini Complete Protease Cocktail Inhibitor tablet per 10 mL of compete buffer (Roche, Mannheim, Germany). The homogenized samples were incubated on ice for 30 min and centrifuged at 10,000 g for 10 min at 4°C. Protein concentration was determined by the Bradford assay, using bovine serum albumin (BSA) as the standard curve (Protein Assay Reagents, Bio-Rad, Hercules, CA). Following protein determination, samples were mixed with Laemmli Sample Buffer (161-0737, Bio-Rad) and 2-mercaptoethanol (Electrophoresis Purity Reagent, 161-0710, Bio-Rad), denatured for 5 minutes at 95°C, and separated on a 4–12% SDS-polyacrylamide gel. The proteins were transferred to PVDF membranes (Millipore, Bedford, MA). The membranes were blocked in PBS with 0.1% Tween-20 (PBS-T) containing 5% non-fat dry milk at room temperature for 1 hour and then washed in PBS-T, incubated with primary antibodies in 5% BSA in PBS-T overnight at 4 C. Membranes were then washed in PBS-T and incubated with horseradish peroxidase-conjugated secondary antibody. After washing in PBS-T, protein detection was performed using SuperSignal West Pico Chemiluminescent Substrate (Pierce, Rockford, IL) and exposed to X-ray film. Antibodies and conditions used were as follows (all antibodies were obtained from Santa Cruz Biotechnology, Santa Cruz, CA): mouse monoclonal to STAT3 (F-2, SC-8019, 1:400), mouse monoclonal to p-STAT-3 (SC-8059, 1:400), goat polyclonal to IL-6 (SC-1265, 1:400), goat polyclonal to IL-1 β (SC-1251, 1:400), goat polyclonal to TNF- α (SC-1350, 1:200). The molecular weight of the detected protein was verified with a commercial standard kit (Prestained SDS-PAGE Standards, 161-0318, Bio-Rad). Three separate immunoblots were used for each sample. Quantification of band density was performed using Quantity One software (Bio-Rad, version 4.4.0) with GAPDH as internal control.

Cardiac tissue cytokine mRNA expression

Total RNA was isolated from frozen heart tissues with RNeasy Minikit (Qiagen, Valencia, CA), subjected to DNase I (Qiagen) treatment. Reverse transcription reactions were performed with 10 μ g of total RNA for each 100- μ l RT reaction with a high capacity cDNA reverse transcription kit (Cat. No 4368814, Applied Biosystems, Foster City, CA) per protocol. Gene

expression of TNF- α and IL-1 β were measured using gene-specific TaqMan assay kits (Applied Biosystems) and a real-time PCR system (IQ 5, Bio-Rad, Hercules, CA) with an optical detection and analysis system. All gene expression levels were expressed as relative changes over the 2 MO WT sham mice, using β -actin as a housekeeping gene. TaqMan assays of β -actin, IL-6, TNF- α , and IL-1 β were purchased as pre-optimized kit from Applied Biosystems with the assay ID Mm00607939_s1, Mm99999068_m1, and Mm01336189_m1, respectively.

Data were expressed as mean \pm standard error of the mean. Comparisons were made between Sham and B+S injury (with the same age and gene), between 2 MO and 14 MO mice (with the same gene and injury), and between WT and KO (with the same age and injury) with t test. A value of $p < 0.05$ was considered statistically significant.

Results

1. Global hemodynamics and cardiac contractile function 24 hours after sham or B+S injury

As previously demonstrated in 2 MO mice, B+S causes marked changes in global hemodynamic and cardiac contractile changes, with a decrease in HR, CO, and an elevated SVR, and relatively maintained MAP; cardiac contractility decreases as shown by load-insensitive variables (ESPVR, PRSW, and E_{\max}) [11,14]. Data in our current study with new 2 MO mice confirmed these findings. In addition, they showed no significant functional changes associated with aging or IL-6 deficiency *per se* in the absence of B+S injury. Consistent with our previous findings, B+S injury caused a significant deterioration of hemodynamic and cardiac contractile function in all mice. In 2 MO mice, IL-6 deficiency was partially protective of cardiac function in terms of higher HR, CO, lower SVR, and higher ESPVR, PRSW, and E_{\max} (Table 1). At 14 months of age, neither WT nor KO mice showed a significant change in the hemodynamic and cardiac function with sham injury alone. After the B+S injury, however, 14 MO mice had worsened hemodynamic and cardiac contractile function compared to the 2 MO counterparts. In addition to the more pronounced decrease in HR and CO, MAP started to decrease despite an elevated SVR. Unlike the 2 MO age group, 14 MO KO mice showed worsened hemodynamic and cardiac contractile function compared to 14 MO WT mice: there were more significant bradycardia, hypotension, low cardiac output; ESPVR, PRSW, and E_{\max} showed markedly decreased contractility (Table 1).

2. p-STAT-3 levels 24 hours after sham or B+S injury

Phosphorylation of STAT-3 occurs following ligand-receptor coupling of IL-6 related cytokines [22], and phosphorylated STAT-3 (p-STAT-3) has been used to indicate IL-6 signal transduction [23]. The ratio of p-STAT-3 to total STAT-3 (p-STAT-3/STAT-3) was used to indicate the level of STAT-3 activation. In 2 MO WT mice, STAT-3, p-STAT-3, as well as p-STAT-3/STAT-3 ratio all increased in response to B+S injury (Figure 1A-C, first pair of bars). At baseline, 2 MO KO mice had a higher level of STAT-3 levels than the 2 MO WT mice, but their p-STAT-3 level as well as the p-STAT-3/STAT-3 ratio remained very low. After B+S injury, there was a significant phosphorylation of STAT-3 which was similar to 2 MO WT mice (Figure 1B-C, second pair of bars). With aging, 14 MO WT mice had a higher level of STAT-3 at baseline, but p-STAT-3 level as well as the p-STAT-3/STAT-3 ratio also remained very low (Figure 1A-C, third pair of bars). After B+S injury, there was a pronounced phosphorylation with a much higher p-STAT-3 level and p-STAT-3/STAT-3 ratio in 14 MO mice than 2 MO mice (Figure 1B-C, first and third pairs of bars). At baseline, 14 MO KO mice had similar p-STAT-3 and p-STAT-3/STAT-3 ratio to 14 MO WT mice; after B+S injury, phosphorylation of STAT-3 was partially attenuated compared to 14 MO WT mice (Figure 1A-C, third and fourth pairs of bars).

3. mRNA production and protein levels of IL-6, TNF- α , and IL-1 β 24 hours after sham or B+S injury

Aging itself was associated with an increase in IL-6 mRNA production in the heart, as evidenced by a greater than 10-fold increase in tissue IL-6 mRNA levels in the 14 MO group over the 2 MO group after sham injury (Figure 2A). After B+S injury, there was a significant increase in cardiac IL-6 mRNA production in both 2 MO and 14 MO mice, but there were no differences in mRNA response between the age groups (Figure 2A). Protein levels of IL-6 in the myocardial tissue, however, were similar among all groups (Figure 2B). IL-6 deficient mice produced no IL-6 mRNA (data not shown), so IL-6 protein was not assayed.

Aging was also associated with an increase in TNF- α mRNA production. In the 14 MO KO group, cardiac TNF- α expression after sham injury was higher than the 14 MO WT group. After B+S injury, TNF- α expression increased in all groups except 14 MO KO whose baseline expression levels were already the highest among all groups and the response after B+S did not significantly increase compared to the sham group at the same age (Figure 3A). Protein levels of TNF- α , however, were similar among all groups, and showed no significant response to B+S injury (Figure 3B).

Much like TNF- α , cardiac IL-1 β mRNA increased with aging after sham injury. After B+S injury, there was a significant increase in IL-1 β mRNA in all groups except in the 14 MO KO mice whose baseline expression levels were highest among all groups and the response after B+S did not significantly increase compared to the sham group at the same age (Figure 4A). IL-1 β protein was higher in the 14 MO WT mice than 2 MO WT mice. In 14 MO KO mice, such a change was attenuated. Changes associated with the B+S injury, however, were not significant (Figure 4B).

Discussion

While our previous studies indicated a role of IL-6 in exacerbating myocardial dysfunction [10][11], current findings in different age groups are somewhat surprising, and possibly contradictory to our hypothesis: 1) Despite increased pro-inflammatory cytokine mRNA expression, 14 MO mice showed no dysfunction until they are injured; 2) IL-6 deficiency protects cardiac function in 2 MO mice but worsens it in 14 MO mice following B+S injury; 3) total body IL-6 deficiency is not necessarily associated with a low STAT-3 or p-STAT-3 level, and phosphorylation of STAT-3 takes place after B+S independent of the IL-6 gene; and 4) IL-6 deficiency is associated with increases in TNF- α and IL-1 β mRNA but not protein production.

The fact that non-injured 14 MO mice exhibit normal cardiac function despite abnormal mRNA production of IL-6, TNF- α , and IL-1 β may indicate existence of compensatory mechanisms to overcome potential detrimental effects of these cytokine transcription abnormalities at this age. In addition, the lack of differences in protein concentrations of these cytokines may indicate possible post-transcriptional regulation that equalizes protein levels despite differences in transcriptional activities. We have previously shown that even in transgenic mice over-producing myocardial IL-6 and increased basal inflammation, cardiac dysfunction did not exist as long as these mice were not injured [11]. It appeared that baseline mRNA transcription abnormalities in 14 MO mice were not associated with cardiac dysfunction. Older mice may ultimately show age-related functional differences as demonstrated by Yang et al using the same method of functional analysis as our study [24].

In contrast to the non-injured state, B+S injury evoked worsened cardiac dysfunction, and such dysfunction was more pronounced in the 14 MO mice than the 2 MO mice. This phenomenon may reflect an additive effect of injury-elicited cytokine activation and the existing altered

gene expression in older mice. The functional difference is in accordance with the clinical finding that outcomes after burns are worse in persons older than 50 years of age [9] despite overtly normal functionality without the injury in most people at this age.

The previously demonstrated beneficial effect of IL-6 deficiency on myocardial function in 2 MO mice [11] was not observed in the 14 MO mice. In fact, IL-6 deficiency worsens cardiac dysfunction in older mice after B+S injury. This finding contrasts with the demonstration of attenuated acute phase reactions and improved survival in 18–20 MO mice after sepsis induced by endotoxin injection [25]. While such a difference in outcome could be attributed to the different injury models and ages used, our data with elevated myocardial levels of p-STAT-3 in IL-6 KO mice after B+S injury suggest that certain functions of IL-6 may be shared by other substances, allowing the gp130-STAT-3 pathway to be activated in the absence of IL-6. The ability of STAT-3 to be phosphorylated and the increase in TNF- α and IL-1 β mRNA production in IL-6 KO mice may serve as evidence of the functional redundancy both within and outside the IL-6 family of cytokines. It is possible that a compensatory mechanism exists in the absence of IL-6, due to the functional redundancy of IL-6 family of cytokines. Such a postulation is in agreement with the fact that IL-6 KO mice manifest no significant structural or functional limitations despite the role of IL-6 in a wide range of biological functions including tissue and organ growth.

Despite IL-6 deficiency, STAT-3 phosphorylation remained intact after B+S injury at either age. In addition, IL-6 deficiency was associated with different mRNA production patterns of pro-inflammatory cytokines at different ages: TNF- α and IL-1 β mRNA levels were higher in 14 MO mice than 2 MO mice, and TNF- α mRNA level is higher in KO than WT mice at this age. The increase in TNF- α and IL-1 β mRNA may reflect a pro-inflammatory change which may play a role in the poor cardiac function in 14 MO KO mice.

Currently, we have no satisfactory explanation for the discrepancy between cytokine mRNA and protein levels. As pointed out in a survey [26], high throughput mRNA assays have different sensitivities and noise levels from the traditional protein assays, and protein measurements are subject to post-transcriptional regulation and varying half-lives of proteins. The Western blot technique may have obscured some potential differences in protein production. Other investigators have also highlighted the importance of post-transcriptional cytokine regulation [27] [28]. The present study design prevented us from taking serial blood samples or applying more sensitive protein assay measurements, such as ELISA of supernatant of cultured myocardial cells, making it possible for us to have “missed” certain significant windows of protein production.

In summary, burn plus sepsis injury causes marked cardiac dysfunction. The role of IL-6 after such an injury appears to be complex and varies with age. IL-6 deficiency is partially protective of cardiac function in 2 MO mice, but is harmful in 14 MO mice. Aging itself is associated with baseline changes in cytokine mRNA levels, and IL-6 deficiency further accentuates these changes. In addition, the STAT-3 activation pathway remains intact after the complex injury even in the absence of IL-6. Cardiac function after burn and sepsis injuries may represent a complex interplay of aging-related cytokine interactions both within and outside the IL-6 family.

Acronyms

TNF- α	Tumor necrosis factor- α
IL-1 β	Interleukin-1 β
IL-6	Interleukin-6

WT	Wild type
KO	IL-6 knockout
MO	Month-old
B+S	Burn complicated by sepsis
TBSA	Total body surface area
STAT-3	signal transducer and activator of transcription 3
p-STAT-3	phosphorylated signal transducer and activator of transcription 3
HR	Heart rate
MAP	Mean arterial pressure
SV	Stroke volume
CO	Cardiac output
SVR	Systemic vascular resistance
ESPVR	Systolic pressure-volume relationship
PRSW	Preload-recruitable stroke work
E_{\max}	Maximum elastance
IVC	Inferior vena cava

References

1. Kishimoto T. Interleukin-6: from basic science to medicine--40 years in immunology. *Annu Rev Immunol* 2005;23:1–21. [PubMed: 15771564]
2. Remick DG, Bolgos G, Copeland S, Siddiqui J. Role of interleukin-6 in mortality from and physiologic response to sepsis. *Infect Immun* 2005;73(5):2751–2757. [PubMed: 15845478]
3. Franceschi C, Bonafe M, Valensin S, Olivieri F, De Luca M, Ottaviani E, De Benedictis G. Inflammaging. An evolutionary perspective on immunosenescence. *Ann NY Acad Sci* 2000;908:244–254. [PubMed: 10911963]
4. Kiecolt-Glaser JK, Preacher KJ, MacCallum RC, Atkinson C, Malarkey WB, Glaser R. Chronic stress and age-related increases in the proinflammatory cytokine IL-6. *Proc Natl Acad Sci USA* 2003;100(15):9090–9095. [PubMed: 12840146]
5. Harris TB, Ferrucci L, Tracy RP, Corti MC, Wacholder S, Ettinger WH Jr, Heimovitz H, Cohen HJ, Wallace R. Associations of elevated interleukin-6 and C-reactive protein levels with mortality in the elderly. *Am J Med* 1999;106(5):506–512. [PubMed: 10335721]
6. McGill V, Kowal-Vern A, Gamelli RL. Outcome for older burn patients. *Arch Surg* 2000;135(3):320–325. [PubMed: 10722035]
7. Pruitt, BA., Jr; Goodwin, CW.; Mason, AD., Jr; Herndon, DN. *Total Burn Care*. Vol. 2. London: W.B. Saunders; 2002. Epidemiological, demographic, and outcome characteristics of burn injury; p. 16-30.
8. Pereira CT, Barrow RE, Sterns AM, Hawkins HK, Kimbrough CW, Jeschke MG, Lee JO, Sanford AP, Herndon DN. Age-dependent differences in survival after severe burns: a unicentric review of 1,674 patients and 179 autopsies over 15 years. *J Am Coll Surg* 2006;202(3):536–548. [PubMed: 16500259]
9. Fitzwater J, Purdue GF, Hunt JL, O'Keefe GE. The risk factors and time course of sepsis and organ dysfunction after burn trauma. *J Trauma* 2003;54(5):959–966. [PubMed: 12777910]
10. Maass DL, White J, Horton JW. IL-1beta and IL-6 act synergistically with TNF-alpha to alter cardiac contractile function after burn trauma. *Shock* 2002;18(4):360–366. [PubMed: 12392281]

11. Zhang H, Wang HY, Bassel-Duby R, Maass DL, Johnston WE, Horton JW, Tao W. Role of Interleukin-6 in Cardiac Inflammation and Dysfunction after Burn Complicated by Sepsis. *Am J Physiol Heart Circ Physiol* 2007;292(5):H2408–H2416. [PubMed: 17220181]
12. Holm C, Melcer B, Horbrand F, von Donnersmarck GH, Muhlbauer W. The relationship between oxygen delivery and oxygen consumption during fluid resuscitation of burn-related shock. *J Burn Care Rehab* 2000;21(2):147–154.
13. Otero RM, Nguyen HB, Huang DT, Gaieski DF, Goyal M, Gunnerson KJ, Trzeciak S, Sherwin R, Holthaus CV, Osborn T, et al. Early goal-directed therapy in severe sepsis and septic shock revisited: concepts, controversies, and contemporary findings. *Chest* 2006;130(5):1579–1595. [PubMed: 17099041]
14. Tao W, Maass DL, Johnston WE, Horton JW. Murine in vivo myocardial contractile dysfunction after burn injury is exacerbated by pneumonia sepsis. *Shock* 2005;24(5):495–499. [PubMed: 16247338]
15. White J, Thomas J, Maass DL, Horton JW. Cardiac effects of burn injury complicated by aspiration pneumonia-induced sepsis. *Am J Physiol Heart Circ Physiol* 2003;285(1):H47–H58. [PubMed: 12637356]
16. Turnbull IR, Wlzonek JJ, Osborne D, Hotchkiss RS, Coopersmith CM, Buchman TG. Effects of age on mortality and antibiotic efficacy in cecal ligation and puncture. *Shock* 2003;19(4):310–313. [PubMed: 12688540]
17. Tao W, Deyo DJ, Traber DL, Johnston WE, Sherwood ER. Hemodynamic and cardiac contractile function during sepsis caused by cecal ligation and puncture in mice. *Shock* 2004;21(1):31–37. [PubMed: 14676681]
18. White J, Maass DL, Giroir B, Horton JW. Development of an acute burn model in adult mice for studies of cardiac function and cardiomyocyte cellular function. *Shock* 2001;16(2):122–129. [PubMed: 11508864]
19. Sherwood ER, Lin CY, Tao W, Hartmann CA, Dujon JE, French AJ, Varma TK. β 2-microglobulin knockout mice are resistant to lethal intra-abdominal sepsis. *Am J Respir Crit Care Med* 2003;167(12):1641–1649. [PubMed: 12626348]
20. Tao W, Sherwood ER. Beta-2 microglobulin knockout mice treated with anti-ASAI OGM-1 exhibit improved hemodynamics and cardiac contractile function during acute intraabdominal sepsis. *Am J Physiol Regul Integr Comp Physiol* 2004;286(3):R569–R575. [PubMed: 14630624]
21. Georgakopoulos, D.; Kass, DA.; Hoit, BD.; Walsh, RA. Cardiovascular physiology in the genetically engineered mouse. Vol. 2. Boston: Kluwer; 2002. Pressure-volume relations; p. 207-222.
22. Taupin, JL.; Minvielle, S.; Thèze, J.; Jacques, Y.; Moreau, JF. The interleukin-6 family of cytokines and their receptors. In: Thèze, J., editor. *The Cytokine Network and Immune Functions*. 1. New York: Oxford University Press; 1999. p. 31-44.
23. Klover PJ, Zimmers TA, Koniaris LG, Mooney RA. Chronic exposure to interleukin-6 causes hepatic insulin resistance in mice. *Diabetes* 2003;52(11):2784–2789. [PubMed: 14578297]
24. Yang B, Larson DF, Watson R. Age-related left ventricular function in the mouse: analysis based on in vivo pressure-volume relationships. *Am J Physiol* 1999;277(5 Pt 2):H1906–H1913. [PubMed: 10564146]
25. Gomez CR, Goral J, Ramirez L, Kopf M, Kovacs EJ. Aberrant acute-phase response in aged interleukin-6 knockout mice. *Shock* 2006;25(6):581–585. [PubMed: 16721265]
26. Greenbaum D, Colangelo C, Williams K, Gerstein M. Comparing protein abundance and mRNA expression levels on a genomic scale. *Genome Bio* 2003;4(9):117. [PubMed: 12952525]
27. Hamilton TA, Novotny M, Datta S, Mandal P, Hartupee J, Tebo J, Li X. Chemokine and chemoattractant receptor expression: post-transcriptional regulation. *J Leukoc Biol* 2007;82(2):213–219. [PubMed: 17409125]
28. Lu J-Y, Sadri N, Schneider RJ. Endotoxic shock in AUF1 knockout mice mediated by failure to degrade proinflammatory cytokine mRNAs. *Genes Dev* 2006;20(22):3174–3184. [PubMed: 17085481]

Figure 1A

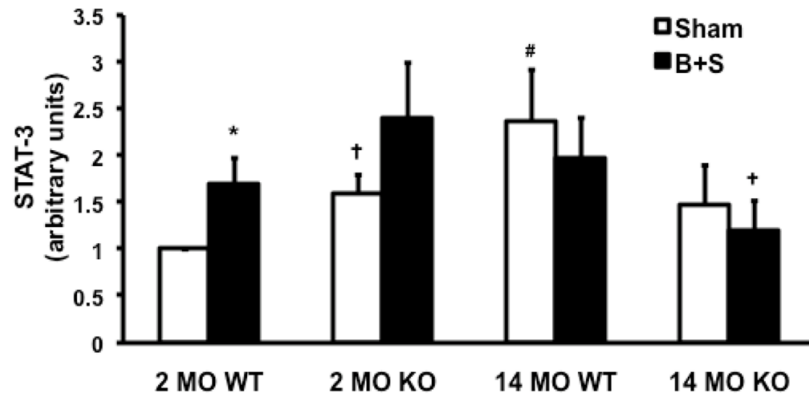


Figure 1B

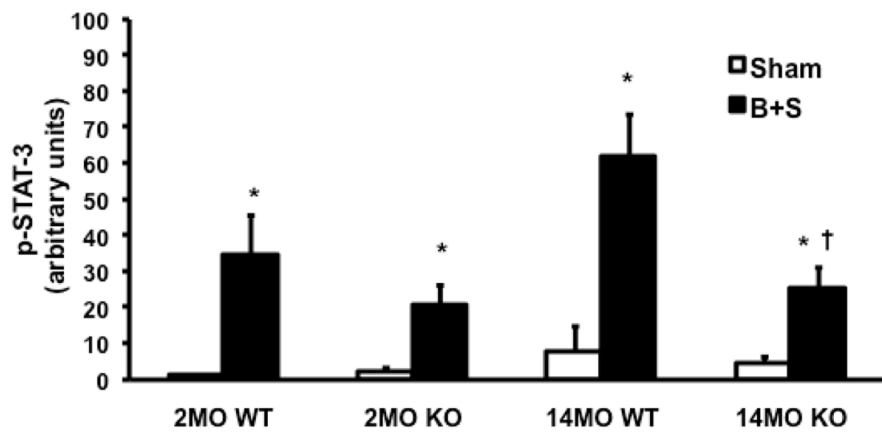


Figure 1C

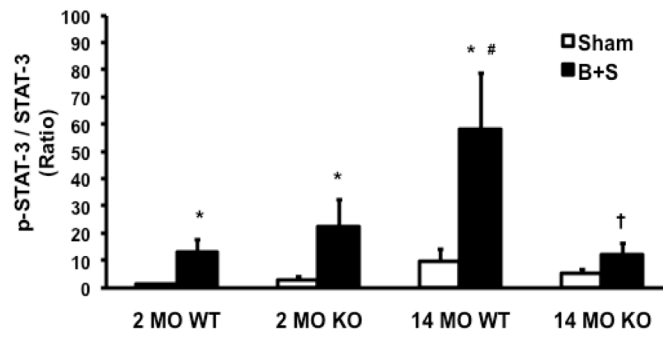
**Figure 1.**

Figure 1A. Levels of STAT-3 in 2 MO and 14 MO WT and KO mice after sham and B+S injury. * $p < 0.05$ vs. sham, # $p < 0.05$ vs. 2 MO, and † $p < 0.05$ vs. WT.

Figure 1B. Levels of p-STAT-3 in 2 MO and 14 MO WT and KO mice after sham and B+S injury. * $p < 0.05$ vs. sham and † $p < 0.05$ vs. WT.

Figure 1C. STAT-3/p-STAT-3 ratio in 2 MO and 14 MO WT and KO mice after sham and B+S injury. * $p < 0.05$ vs. sham, # $p < 0.05$ vs. 2 MO, and † $p < 0.05$ vs. WT.

Figure 2A

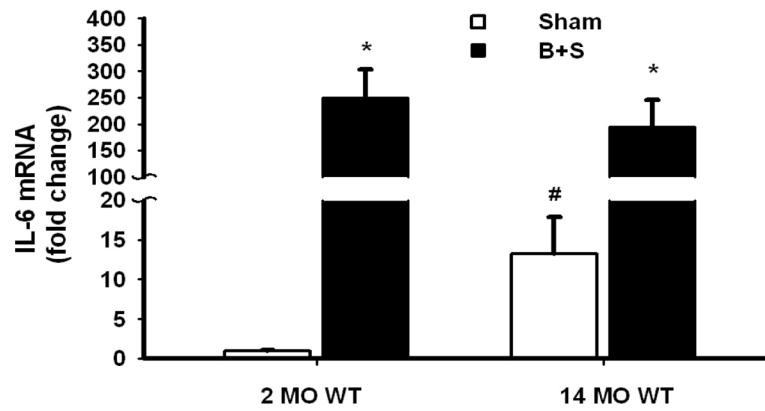


Figure 2B

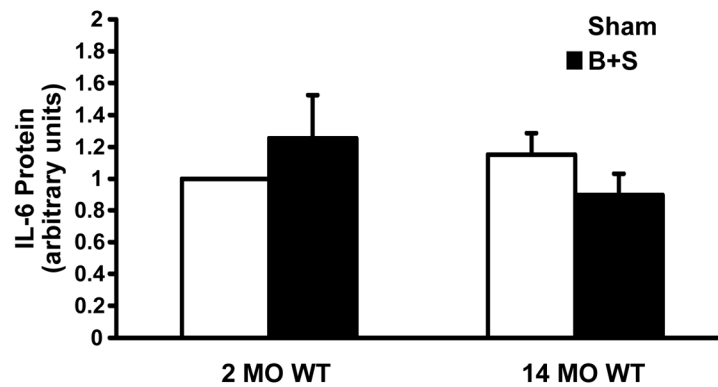
**Figure 2.**

Figure 2A. IL-6 mRNA levels by real-time PCR in 2 MO and 14 MO WT mice after sham and B+S injury. * $p < 0.05$ vs. Sham.

Figure 2B. IL-6 protein levels by Western blot in 2 MO and 14 MO WT mice after sham and B+S injury.

Figure 3A

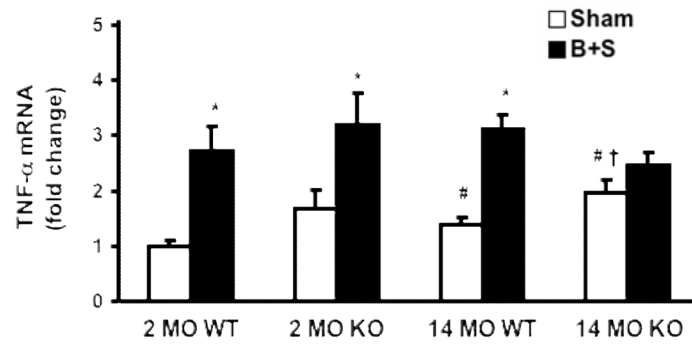


Figure 3B

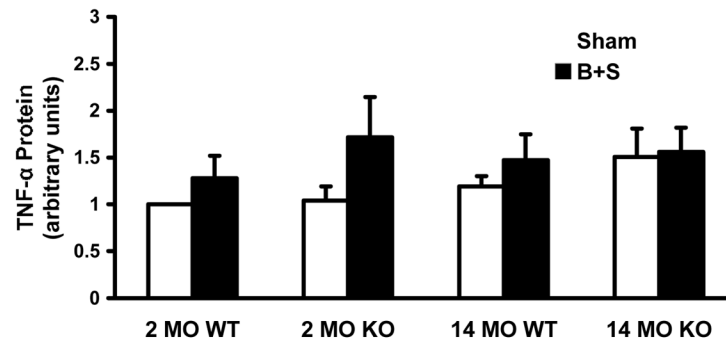
**Figure 3.**

Figure 3A. TNF- α mRNA levels by real-time PCR in 2 MO and 14 MO WT and KO mice after sham and B+S injury. * $p < 0.05$ vs. sham, # $p < 0.05$ vs. 2 MO, and † $p < 0.05$ vs. WT.

Figure 3B. TNF- α protein levels by Western blot in 2 MO and 14 MO WT and KO mice after sham and B+S injury.

Figure 4A

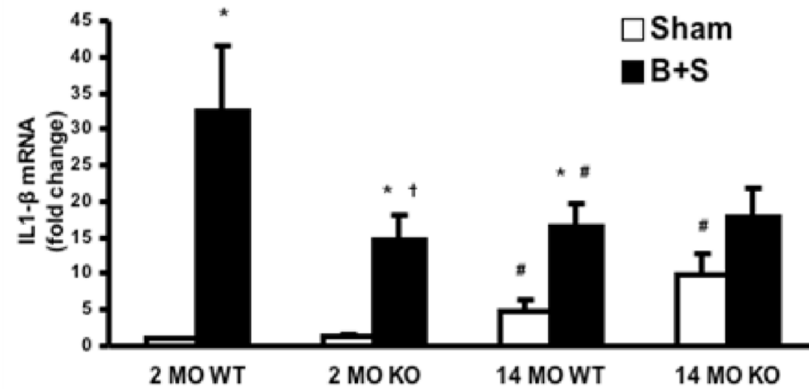


Figure 4B

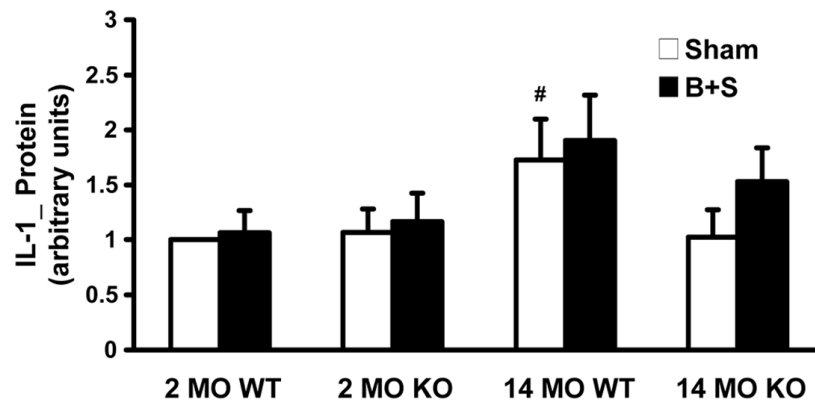
**Figure 4.**

Figure 4A. IL-1 β mRNA levels by real-time PCR in 2 MO and 14 MO WT and KO mice after sham and B+S injury. * $p < 0.05$ vs. sham, # $p < 0.05$ vs. 2 MO, and † $p < 0.05$ vs. WT.

Figure 4B. IL-1 β protein levels by Western blot in 2 MO, 14 MO, WT and KO mice after sham and B+S injury. # $p < 0.05$ vs. 2 MO.

Table 1

Major hemodynamic and cardiac contractile function variables in 2 MO and 14 MO WT and KO mice after burn complicated by sepsis

	2 MO				14 MO			
	Sham		B + S		Sham		B + S	
	WT	KO	WT	KO	WT	KO	WT	KO
<u>Steady-State</u>								
HR	557 ± 8	562 ± 8	495 ± 7*	539 ± 7 [†]	556 ± 10	564 ± 12	439 ± 21**	378 ± 20* ^{††}
MAP	84 ± 2	88 ± 3	82 ± 3	84 ± 3	81 ± 4	87 ± 4	63 ± 3**	50 ± 4* ^{††}
CO	9.3 ± 0.3	9.6 ± 0.6	4.9 ± 0.3*	7.4 ± 0.3* [†]	8.5 ± 0.6	8.4 ± 0.3	4.0 ± 0.3**	3.5 ± 0.4* ^{††}
SVR	9.2 ± 0.3	9.6 ± 0.6	17.5 ± 1.0*	11.6 ± 0.6* [†]	9.9 ± 0.6	10.1 ± 0.6	17.2 ± 1.6*	24.5 ± 4.9* ^{††}
<u>IVC Occlusion</u>								
ESPVR	20.7 ± 2.8	22.6 ± 3.0	4.6 ± 0.8*	6.9 ± 0.8* [†]	17.5 ± 3.0	15.5 ± 2.6	2.8 ± 0.3**	1.9 ± 0.3* ^{††}
PRSW	104 ± 5	108 ± 5	37 ± 2*	77 ± 4* [†]	92 ± 7	89 ± 9	30 ± 3**	22 ± 2* ^{††}
E _{max}	39.7 ± 2.1	41.3 ± 2.3	18.0 ± 1.5*	26.8 ± 2.9* [†]	35.4 ± 2.4	34.8 ± 1.8	13.7 ± 1.5**	8.9 ± 0.9* ^{††}

HR: heart rate (beats per minute); MAP: mean arterial pressure (mmHg); CO: cardiac output (mL/min); SVR: systemic vascular resistance (mmHg/mL/min); ESPVR: end-systolic pressure volume relationship (mmHg/ μ L); PRSW: preload-recruitable stroke work (mmHg- μ L); E_{max}: maximum elastance (mmHg/L). Data are expressed as mean \pm SEM.

* p < 0.05 between sham and B+S

p < 0.05 between 2 MO and 14 MO mice, and

[†] p < 0.05 between WT and KO.